

– SUPPORTING INFORMATION –

**Quantum-confined GaN Nanoparticles Synthesized via
Liquid-Ammonia-in-Oil-Microemulsions**

Fabian Gyger^a, Pascal Bockstaller^b, Henriette Gröger^a, Dagmar Gerthsen^b, Claus Feldmann^{a*}

^a Institut für Anorganische Chemie,
Karlsruhe Institute of Technology (KIT)
Engesserstrasse 15, 76131 Karlsruhe, Germany

^b Laboratorium für Elektronenmikroskopie
Karlsruhe Institute of Technology (KIT)
Engesserstrasse 7, 76131 Karlsruhe, Germany

1. Analytical tools

General: All analytical data and sample handling was performed under inert conditions (nitrogen or argon) in order to avoid contact to moisture and oxygen.

Scanning electron microscopy (SEM) and scanning transmission electron microscopy (STEM): SEM/STEM were performed with a Zeiss Supra 40 VP, equipped with a field emission gun (acceleration voltage 4-20 kV, working distance 2-4 mm). The GaN nanoparticles were prepared on Si wafers by evaporation of a freshly prepared suspension in ethanol.

Transmission electron microscopy (TEM): Transmission electron microscopy (TEM), scanning transmission electron microscopy (STEM) and high-resolution transmission electron microscopy HRTEM were conducted with an aberration-corrected FEI Titan³ 80-300 microscope at 300 kV. TEM samples were prepared by evaporating chloroform- or ethanol-based suspensions on amorphous carbon (Lacey-)film suspended on copper grids. The deposition of the samples on the carbon (Lacey-)film copper grids was performed under Argon atmosphere in a glove-box. The grids were thereafter transferred with a suitable vacuum/inert gas transfer module into the transmission electron microscope without any contact to air. Average particle diameters were calculated by statistical evaluation of at least 150 particles (Scandium 5.0 software package, Soft Imaging Systems).

X-ray powder diffraction (XRD): X-ray powder diffraction (XRD) was performed with a Stoe STADI-P diffractometer operating with Ge-monochromatized Cu-K α -radiation ($\lambda = 1.54178 \text{ \AA}$) and Debye-Scherrer geometry.

Infrared Spectroscopy (FT-IR): Fourier-transform infrared spectra were recorded on a Bruker Vertex 70 FT-IR spectrometer using KBr pellets.

Optical spectroscopy (UV-VIS): Diffuse reflectance spectra of the as-prepared GaN powders were recorded in a wavelength interval of 250–800 nm with a Varian Cary 100 spectrometer, equipped with an integrating sphere against BaSO₄ as a reference.

Fluorescence spectroscopy (FL): Emission spectra were recorded with a Jobin Yvon Spex Fluorolog 3 equipped with a 450 W Xe-lamp and double grating excitation and emission monochromators.

2. Use of heptane suspensions for depositing GaN thin-films

After acetonitrile-driven phase separation and removal of most of the surfactants, the remaining heptane top-phase containing the GaN nanoparticles can be used for depositing GaN thin-films. According to dynamic light scattering (DLS) the as-prepared GaN nanoparticles in heptane exhibit a mean diameter of 3.3 nm at narrow size distribution (Figure S1). Moreover, these suspensions turned out as colloidally stable for several weeks without any considerable agglomeration. Colloidally stable suspensions of crystalline GaN can be highly interesting for layer deposition and thin-film printing for semiconductor applications, including LEDs as well as solar cells. Notably, colloidally stable GaN suspensions can be hardly obtained via synthesis strategies that require elevated temperatures (200–900 °C) for preparation and/or crystallization of GaN.

As a first conceptual study, a GaN thin-film was obtained by dropping the as-prepared GaN nanoparticle suspension in heptane on a silicon substrate. Subsequent slow solvent evaporation resulted in a comparably dense GaN film with a thickness of about 100 nm (Figure S1). However, much more detailed studies are necessary to optimize the film deposition as well as its thickness and density. This topic is beyond the focus of the current investigation.

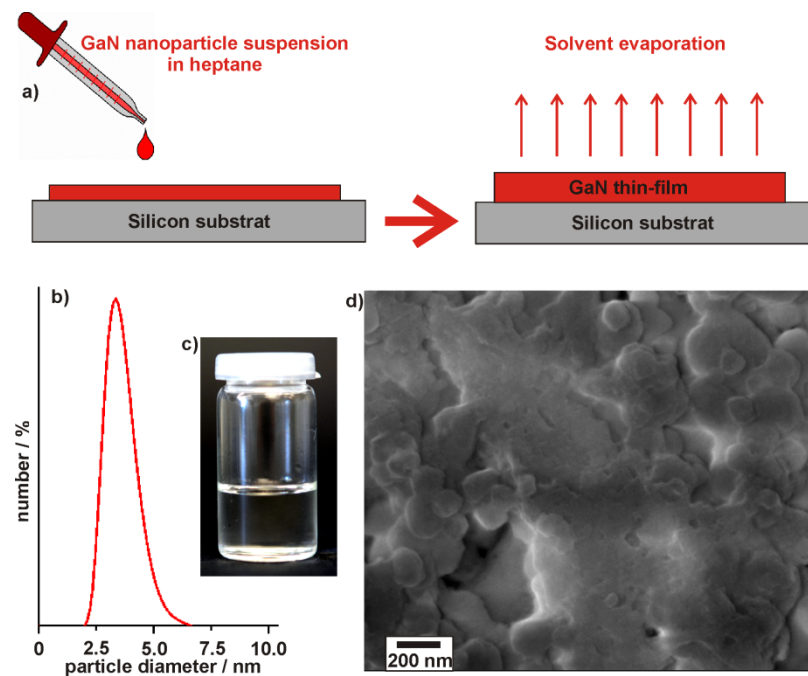


Figure S1. Scheme displaying: a) conceptual thin-film manufacturing with the as-prepared GaN nanoparticles; b) Particle size and size distribution of a suspension of GaN in heptane according to dynamic light scattering; c) Photo of a suspension of the as-prepared GaN nanoparticles in heptane; d) Scanning electron microscopy of a GaN thin-film on a silicon substrate.

3. Electron microscopic characterization

Figure 3 (*cf. main manuscript*) as well as Figure S2 (STEM), Figure S3 (TEM), Figure S4 (HRTEM) show electron microscopy images of some tens of individual GaN nanoparticles at different magnification and contrast (individual nanoparticles are indicated by red circles). Notably, the contrast of the nanoparticles (due to the absorption of the electron beam) and the intensity of the lattice fringes (due to the scattering power of the nanoparticles) are both weak. Taking the small particle size (3–4 nm) and the low molar weight (84 g/mol) of GaN into account, this finding is to be expected. Moreover, it has to be considered that the GaN nanoparticles are deposited on Lacey-carbon films as the sample holder in the electron microscope. This carbon film also has a certain thickness causing certain absorption of the electron beam. Both thickness and absorption of the carbon film are very low but in view of 3–4 nm-sized GaN nevertheless considerable. As a consequence, the contrast of the GaN nanoparticles on the carbon film has to be expected to be considerably lower as, for instance, in the case of nanosized gold particles.

Based on various images that were taken with different electron microscopy techniques (STEM: Figure S2), (TEM: Figure S3), (HRTEM: Figure S4), the size and size distribution of the as-prepared GaN nanoparticles is reliably evidenced. On the other hand, electron microscopy as a matter of course only shows a limited number of nanoparticles on one image. In order to investigate a statistically relevant number of nanoparticles, dynamic light scattering of GaN suspensions is highly relevant as well (*cf. main manuscript: Figure 2*). If all these independent analytical tools – STEM, TEM, HRTEM, DLS – coincide in view of particle size and size distribution, both are reliably proven.

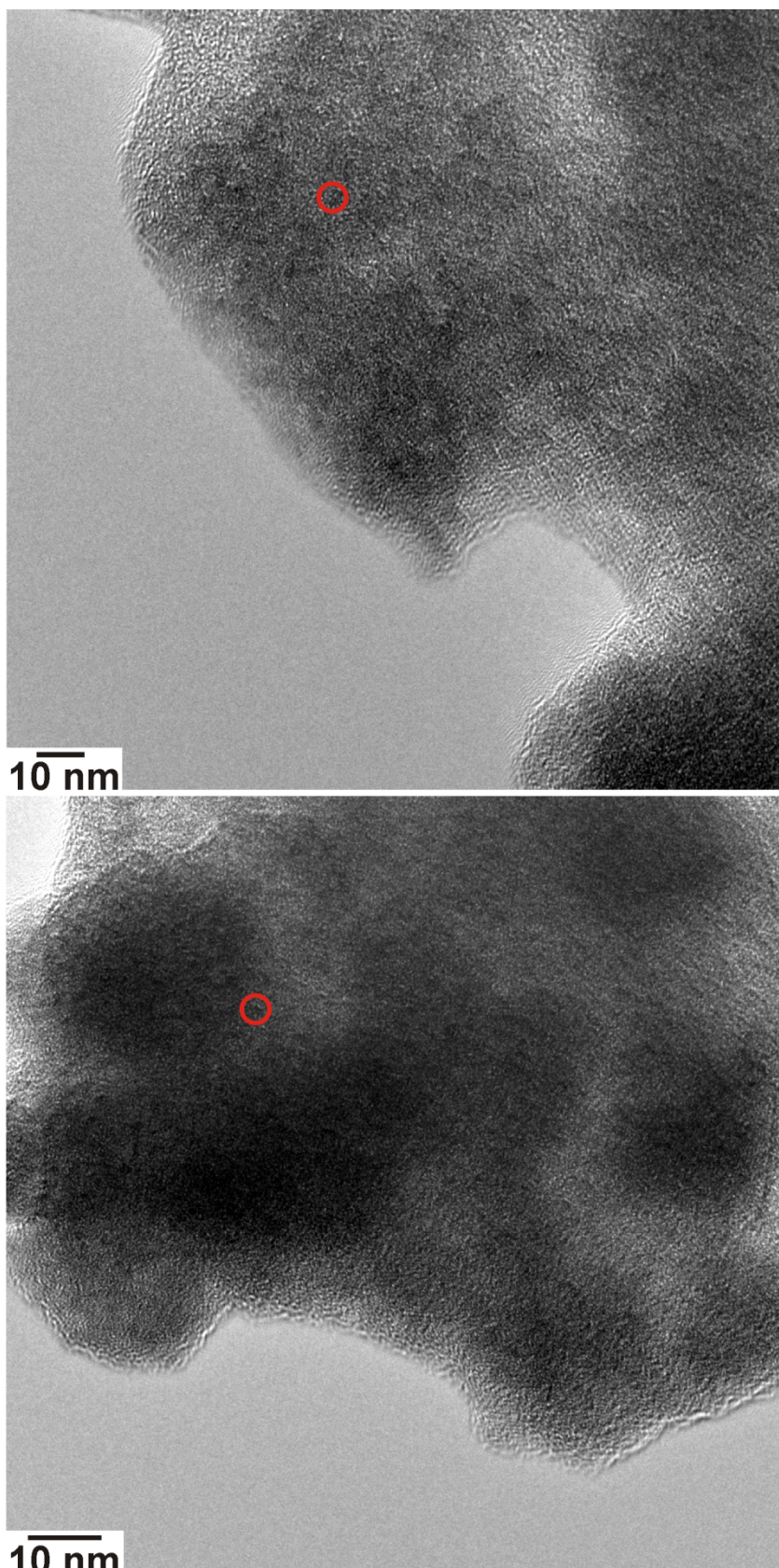


Figure S2. STEM images of the as-prepared GaN nanoparticles (individual nanoparticles exemplarily indicated by red circles; deposited on Lacey carbon copper grid).

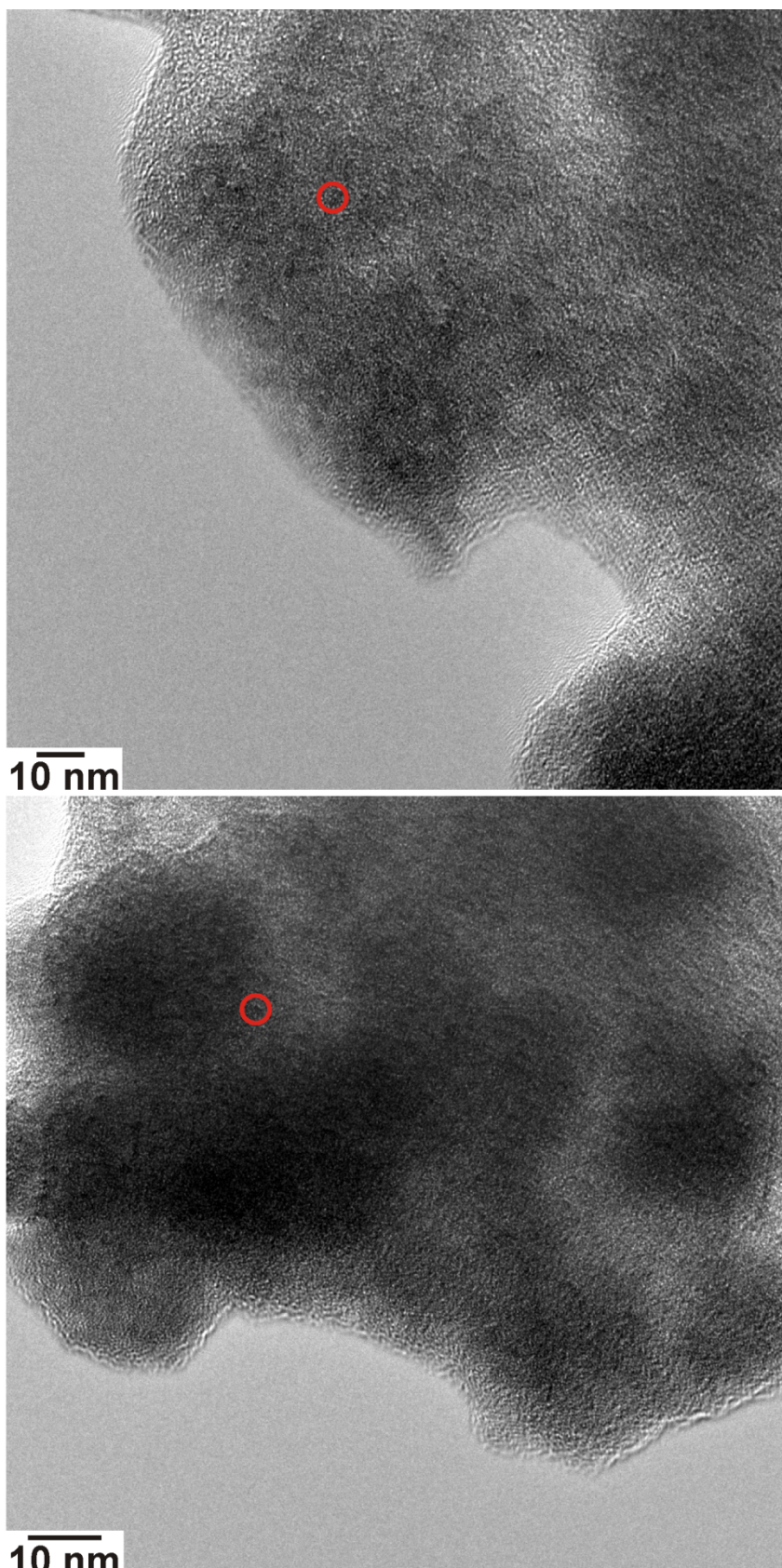


Figure S3. TEM images of the as-prepared GaN nanoparticles (individual nanoparticles exemplarily indicated by red circles; deposited on Lacey carbon copper grid).

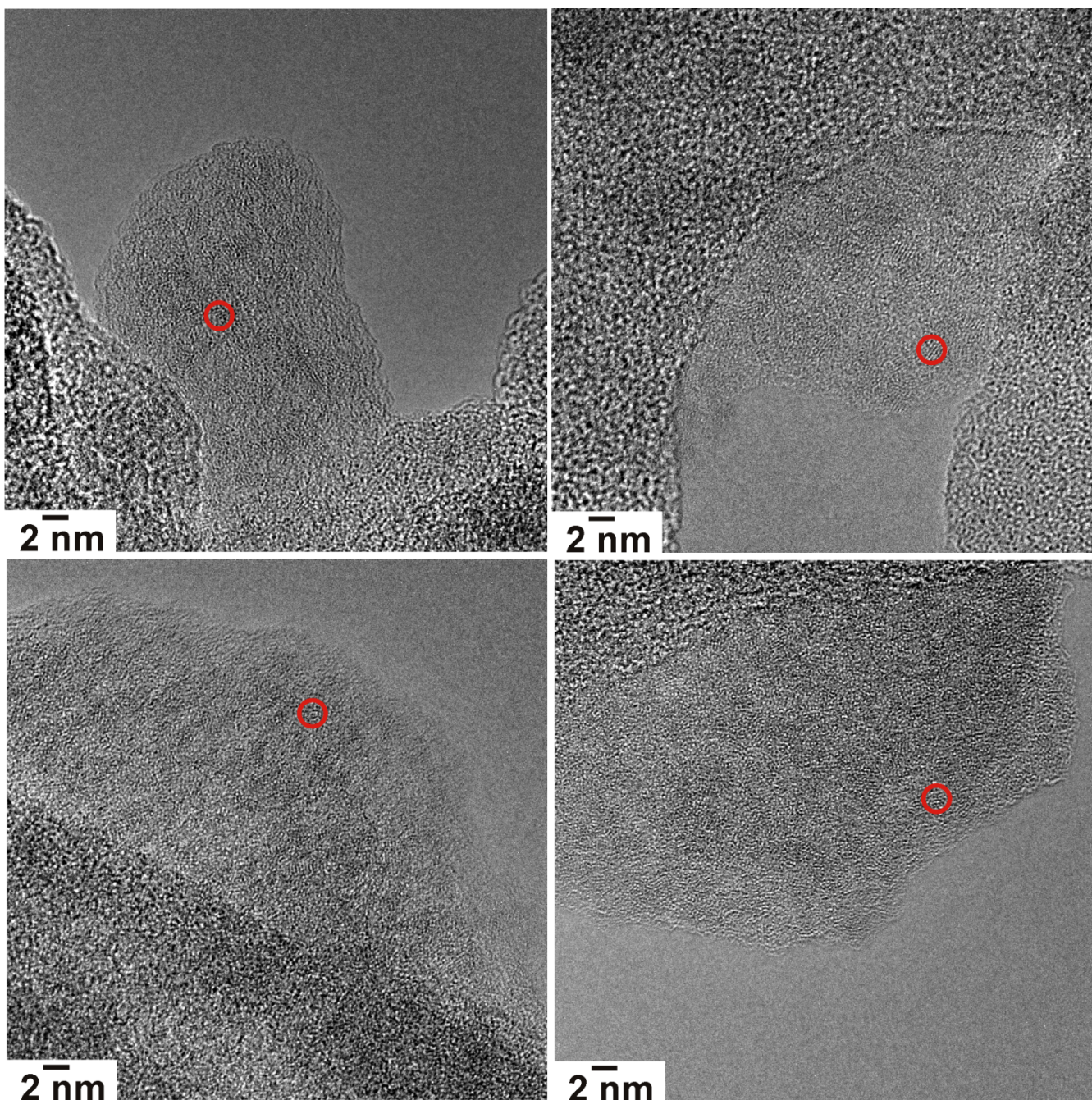


Figure S4. HRTEM images of the as-prepared GaN nanoparticles (individual nanoparticles exemplarily indicated by red circles; deposited on Lacey carbon copper grid).

4. X-ray powder diffraction analysis

Due to the small particle size (3–4 nm), the Bragg peaks of the as-prepared GaN nanoparticles are very broad and low in intensity (*cf. main manuscript: Figure 4a*). Taking the (111) Bragg peak at 35 ° of 2-Theta as an example, the full-width-at-half-maximum (FWHM) with a value of about 2.8–3.4 ° –

according to the Scherrer equation – relates to a crystallite size of 3.0–3.5 nm. This is well in accordance to the observed particle size of 3–4 nm. Due to the small particle size and the resulting lattice distortion, the lattice parameters of the nanoparticles are slightly larger as compared to infinite bulk-GaN given as a reference. Consequently, all Bragg peaks are slightly shifted to lower 2-Theta values. Due to the limited number of Bragg peaks of cubic GaN as well as due to the low intensity and broad peak width, calculating the particle size via the Scherrer equation is of limited significance here. Therefore, the procedure is not discussed in detail. In addition, electron microscopy (*cf. main manuscript: Figure 3*) and dynamic light scattering (*cf. main manuscript: Figure 2*) are used to determine the particle diameter with much higher significance.

As the scattering power of the as-prepared GaN nanoparticles is low, the non-specific background of the XRD measurement (e.g., due to glass capillary as sample holder, small-angle scattering of nanoparticles, non-specific scattering of XRD equipment) seemingly is high although the absolute intensity is very low. For comparison, a glass capillary filled with amorphous glass powder is shown in Figure S5 that also shows a non-specific broad peak around 22 ° of 2 Theta (indicated by *). As the crystallinity of the GaN nanoparticles increases after sintering at elevated temperatures, the Bragg peaks of GaN become more intense. Although still at similar absolute intensity, the non-specific background in comparison is now becoming very weak. Notably, the additional sharp Bragg peaks (indicated by #) observed after sintering at 800 °C relate to hexagonal α -GaN and the beginning phase transformation from cubic β -GaN to α -GaN.^{4,5}

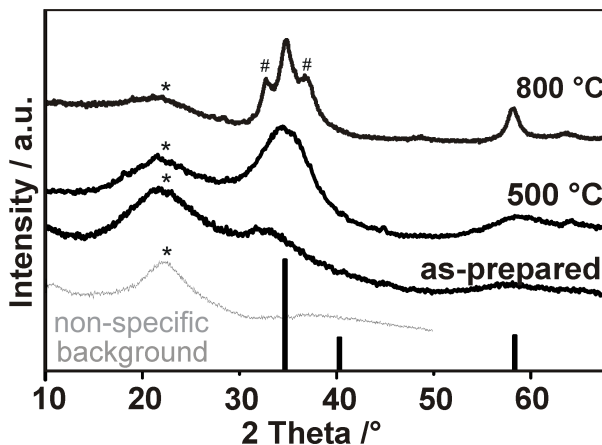


Figure S5. XRD patterns of GaN nanoparticles (as-prepared, sintered at 500 °C, sintered at 800 °C) with glass capillary (filled with amorphous glass powder) as a reference of the non-specific background.

5. Determination of the optical band gap

The optical band gap of the as-prepared GaN nanoparticles was determined from a Tauc-plot (Figure S6). To this concern, the linear region in the $(\alpha h\nu)^2$ -versus- $h\nu$ plot was fitted. The obtained value of 4.35 eV (289 nm) for the band gap of the as-prepared β -GaN is in good agreement with previously reported data of β -GaN nanoparticles (4.0 to 4.6 eV [1–3]).

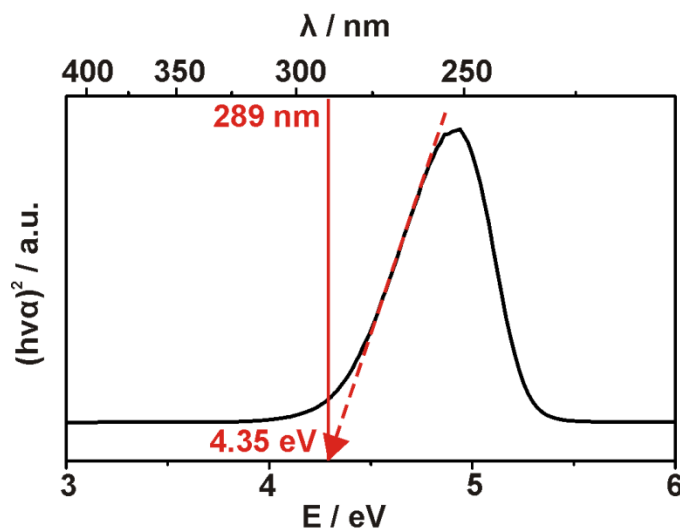


Figure S6. Tauc plot for optical-band-gap determination of the as-prepared GaN nanoparticles.

References

- 1 G. Pan, M. E. Kordesch and P. G. van Patten, *Chem. Mater.*, 2006, **18**, 3915.
- 2 A. C. Frank, F. Stowasser, H. Sussek, H. Pritzkow, C. R. Miskys, O. Ambacher, M. Giersig and R. O. Fischer, *J. Am. Chem. Soc.*, 1998, **120**, 3512.
- 3 R. L. Wells and J. F. Janik, *Eur. J. Solid State Inorg. Chem.*, 1996, **33**, 1079.
- 4 A. F. Wright and J. S. Nelson, *Phys. Rev. B*, 1995, **51**, 7866.
- 5 C. Balkas, C. Basceri and R. Davis, *Powder Diffraction*, 1995, **10**, 266.